Adaptive Correction of Radar–tracking Images

Oleg Sytnik

A. Ya. Usikov Institute for Radio Physics and Electronics under the National Academy of Sciences of Ukraine

12, Str. Proskura, Kharkov, Ukraine 61085

ssvp127@gmail.com

***Abstract*-The problem of adaptive correction of the trajectory distortions on the images of the earth's surface, which are formed by synthetic-aperture radar (SAR), is discussed. The proposed method belongs to the class of adaptive self-focusing methods, in which the information on trajectory errors is retrieved from a reflected sounding signal. We have used the estimates of the Doppler spectrum displacement and its high derivatives averaged over the slant range as information parameters. It provided an opportunity to build an adaptive algorithm, which can automatically correct not only flight velocity errors, but acceleration and jump errors as well. The results of SAR signal processing are presented. The features of signal processing under different conditions and implementation of the proposed method are discussed.**

Keywords*- *Coherent Radar; Doppler Spectrum; Distortions; Trajectory Errors; Radar's Image of Surface; Synthetic Aperture Radar (SAR)

I. INTRODUCTION

Onboard synthetic-aperture radar (SAR) provides tracking images of the earth's surface by coherent processing of the sounding signals reflected from the surface [1-2]. The amplitude and phase of the reflected signals contain information about the surface characteristics and objects placed on it. The reflected signals along the tracking trajectory are written in the memory for each strobe of the slant range and then are processed by convolution with a supporting function to produce images. Such a principle of earth-tracking is very effective in aircraft and on board satellite radar to solve many important scientific and practical tasks. An image can be produced onboard and have a very high spatial (azimuthal and slant range) resolution.

The supporting function of the signal processor is apriori built from the assumption that aircraft trajectory is a straight line. Aircraft deviations from the straight line, which are not taken into account in the signal processing algorithm, cause image distortions such as defocusing in azimuth and slant coordinates, object displacement from their real positions, a decrease in the image brightness, an increase in the side lobes of the synthesized antenna and, as a result, the appearance of repeated targets and some other distortions. Therefore, in most cases, if aircraft deviation occurs, in order to obtain a good-quality image, the antenna synthesizing time interval has to be reduced which leads to resolution degradation.

There are many different methods to compensate for those negative effects [3-8]. The numerous methods can be divided into three classes:

a) Information on the SAR trajectory platform position is obtained from special onboard sensors of navigation systems.

b) Information on the SAR trajectory platform position is extracted from sounding signals reflected from the earth's surface.

c) A combination of methods.

The design of the SAR that is invariant to different navigation systems is preferable to the second group of methods. It is exactly these particular methods the present paper is devoted to.

II. PROBLEM STATEMENT

Usually the algorithm of antenna pattern synthesis in SAR can be written as a convolution integral for each strobe of slant range [1]:

$$y(\tau) = \mathrm{mod}\left\{ \int_{-T_c/2}^{T_c/2} \dot{x}\left(t-\tau\right)\dot{h}\left(t\right)dt \right\}, \tag{1}$$

where $\mathrm{mod}\{\cdot\}$ is the modulus of function; T_c is the interval of time during which you are to synthesize an antenna aperture;

$\dot{x}\left(t-\tau\right) = \dot{s}\left(t-\tau\right) + \dot{n}(t)$ is additive sum of the signals, from surface and no coherent noise; the signal is: $\dot{s}\left(t-\tau\right) = A\left(t-\tau\right)e^{-j\left(4\pi r_i(t)/\lambda\right)}$; A is the amplitude of reflected signal; $r_i\left(t\right)$ is the current value of the slant range from the phase center of the transmitting antenna to the i-th point reflector placed on a surface; λ is the wavelength (the factor $\omega_0 t$ has been omitted here); noise is: $\dot{n}(t)$, the variance of noise is σ^2 and its expectation is zero; $\dot{h}\left(t\right) = H\left(t\right)e^{j\left(2\pi v^2 t^2/\lambda r_0\right)}$ is the supporting function, where $H(t)$ is the weighting function which in the simplest case can be $H(t)\equiv 1$; v is the ground speed of motion of the SAR carrier.

Fig. 1 (curve 1) shows the antenna pattern synthesized under ideal conditions when there are no trajectory distortions, which is a result of algorithm (1) processing.

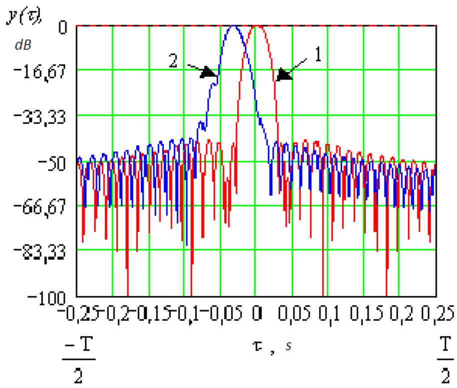

Fig. 1 The antenna pattern synthesized under ideal conditions (curve 1); the antenna pattern synthesized with ground speed and acceleration errors (curve 2)

The curve 2 in Fig. 1 illustrates the type of distortions which appear in synthesized antenna pattern under conditions of non-stationary motion of the SAR platform. It is easy to see that errors in ground speed definition lead to displacement of the maximum of the synthesized antenna pattern or targeting errors. To form both patterns we used the Hamming weighting function [9].

The errors in acceleration and jump (the velocity variation of acceleration) of SAR platform leads to an increase in the main lobe width of the synthesized antenna pattern and to an increase in its side lobes. As a consequence, we have geometrical distortions of the objects on an image, their defocusing, a reduced azimuthal resolution and the emergence of repeated targets on the image.

III. SIGNAL PROCESSING METHOD

The characteristic of variation in a trajectory signal on the interval of synthesis T_c during radiation of a point target on the earth's surface is under the Chirp Law with frequency $\omega = 4\pi v(t)t/(\lambda r_0)$. When ground velocity is $v(t)=const$, the Chirp Law is a linear function and an envelope of its Doppler spectrum is symmetrical, as see in Fig. 2 (curve 1). The errors in definition of platform motion lead to distortions of the Doppler spectrum symmetrical structure (Fig. 2, curve 2). So it seems appropriate to use the analysis of the Doppler spectrum form to correct supporting function in algorithm (1) for automatic correction of trajectory distortions.

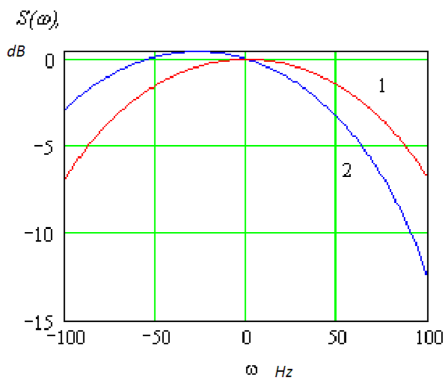

Fig. 2 The idealized envelope of the Doppler spectrum form (curve 1) and shifted envelope of Doppler's spectra form under trajectory distortions (curve 2)

The real reflected signal is highly noisy. As an example, Fig. 3 shows (symbols "+") the trajectory signal spectrum averaged over 128 neighborhood range strobes on the part of trajectory where an aircraft executed maneuvering. Because of high dispersion of the Doppler spectrum envelope samples, it is difficult to construct the procedure for calculating reliable estimates of their shifts and asymmetry coefficients for correcting supporting function in algorithm (1). However, if spectral samples would be approximated by a well-known function, for example, the polynomial function, then the calculation procedure of correcting coefficients can be implemented.

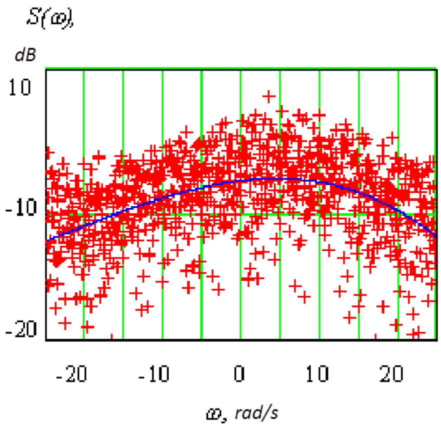

Fig. 3 The spectral density of Doppler trajectory signal frequencies during the air craft maneuvers (shown by symbols "+") and its third-degree polynomial approximation (solid line)

The third-degree polynomial approximation of the Doppler spectrum amplitude envelope with a set of coefficients: 24,469; 0,024; 1,656 * 10-5; -4,507 * 10-8 is shown in Fig. 3 by a solid line. The polynomial coefficients have been calculated from the next system of equations:

$$\sum_{l=0}^{n} c_l \int_{-\omega}^{\omega} g(l,k,\omega)\,d\omega = \int_{-\omega}^{\omega} g(l,k,\omega)\,S(\omega)\,d\omega\,, \tag{2}$$

where $k = 0,1,...,n+1$; n is the polynom's degree; c_l is the coefficient of polynom according to its index; $g(l,k,\omega) = \omega^{l+k-1}$ is the basic function.

Under the criteria of mean-square error, the value of normalized error is $\sigma_p = \sqrt{\dfrac{\sum_{i=0}^{m-1}\left(g(\omega_i) - E\{S(\omega)\}\right)^2}{\sum_{i=0}^{m-1}\left(S(\omega_i) - E\{S(\omega)\}\right)^2}}$, where $E\{\bullet\}$ is the symbol of expectation operator. In our experiments the value of σ_p has been less than 0.248.

Moreover, if one assumes that the SAR platform is not capable of executing the rapid changes in its position relative to the synthesizing interval, and the high-frequency fluctuations caused by platform vibrations are negligible, then in the Maclaurin's expansion into series in terms of the power exponent we can use no more than three terms of the series [6].

Then the instantaneous value of slant range r(t) from the phase center of the real SAR antenna relative to the point reflector on a surface is written as:

$$r_i(t) = r_{\max} + \frac{d \cdot r_i(0)}{dt} \cdot t + \frac{d^2 \cdot r_i(0)}{dt^2} \cdot \frac{t^2}{2} + \frac{d^3 \cdot r_i(0)}{dt^3} \cdot \frac{t^3}{6} + \sum_{\nu=4}^{\infty} \frac{d^{(\nu)} \cdot r_i(0)}{dt^{\nu}} \cdot \frac{t^{\nu}}{\nu!}\,. \tag{3}$$

Using formula (3), it is not difficult calculate the projection of phase errors in the supporting function for aircraft drift along coordinates X, Y, Z, where coordinate X coincides with the flight direction, coordinate Y coincides with the line which is perpendicular to the flight line and coordinate Z is a normal to the ground surface.

$$\begin{aligned} \phi_{tr}(t) = -\frac{4\pi}{\lambda}\{&\left[\Delta X \frac{vt}{r_{\max}} - \Delta Y \sin(\theta) + \Delta Z \cos(\theta)\right] + \\ &+ \left[\frac{v}{r_{\max}}(\Delta X - \Delta X' t) - \Delta Y' \sin(\theta) + \Delta Z' \cos(\theta)\right] t + \\ &+ 0.5\left[\Delta X'' - \Delta Y'' \sin(\theta) + \Delta Z'' \cos(\theta)\right] t^2\}\,, \end{aligned} \tag{4}$$

where ΔX, ΔY, ΔZ are the errors of aircraft position accordingly to X, Y, Z coordinates; $\Delta X'$, $\Delta Y'$, $\Delta Z'$, $\Delta X''$, $\Delta Y''$, $\Delta Z''$ are the corresponding derivatives of these errors; v is aircraft's initial velocity at the moment t; θ is the angle between the normal to ground surface and direction to the target.

The phase error caused by the combined ambiguity of a sideslip angle and the SAR platform position are defined as a series:

$$\phi_\beta(\Delta X(t),\beta(t)) = -\frac{4\pi}{\lambda}(\Delta X\beta + [\Delta X'\beta + \Delta X\beta'] + \frac{1}{2}[\Delta X''\beta + 2\Delta X'\beta' + \Delta X\beta'']t^2\}, \tag{5}$$

where β, β', β'' are the sideslip angle, the velocity of the sideslip angle and the acceleration of the sideslip angle respectively.

The phase error caused by the combined ambiguity of angle θ and the SAR platform position reads as

$$\begin{aligned}\phi_\theta(\Delta Y,\Delta Z) = -\frac{4\pi}{\lambda}\{&\Delta Z\cos\theta - \Delta Y\sin\theta + [\Delta Z'\cos\theta - \Delta Z\theta'\sin\theta - \Delta Y'\sin\theta \\ &-\Delta Y\theta'\cos\theta]t + \frac{1}{2}[\Delta Z''\cos\theta - 2\Delta Z'\theta'\sin\theta - \Delta Z\theta''\sin\theta - \Delta Z\theta'^2\cos\theta - \\ &-\Delta Y''\sin\theta - 2\Delta Y'\theta'\cos\theta - \Delta Y\theta''\cos\theta + \Delta Y\theta'^2\sin\theta]t^2\}.\end{aligned} \tag{6}$$

Now consider in more detail the case where the SAR platform flight velocity is changing on the synthesizing interval. As shown in [4], the phase incursion of a signal from the point reflector to the antenna phase center can be written as:

$$\phi_v(t) = -\frac{2\pi}{\lambda r_0}\cdot\left[v_0 + \Delta v\cdot t + \frac{1}{2}a'\cdot t^2\right]^2\cdot t^2, \tag{7}$$

where v_0, Δv, a' is the SAR platform velocity, its acceleration and acceleration derivative respectively.

In order to correct the signal trajectory distortions in the phase factor of the supporting function it is necessary to take into account the coefficients Δv, a', which are selected by comparing curve 2 (Fig. 3) with reference curve 1 (Fig. 2). To formalize this procedure one can make use of the conjugate gradient method [11]. Let us designate the shifted spectral density as $S_2(\omega)$. The argument $\omega = \omega^*$, which corresponds to extremum ω^* is then calculated through iteration of the procedure

$$\omega^{k+1} = \omega^k - \alpha_k\nabla S_2(\omega^k) + \beta_k(\omega^k - \omega^{k-1}), \tag{8}$$

where the optimal values of coefficients α_k, β_k at each step of the iteration procedure are calculated according to the relation

$$\{\alpha_k,\beta_k\} = \frac{\arg\min}{\{\alpha_k,\beta_k\}}\left\{S\left(\omega^k - \alpha_k\nabla S_2(\omega^k) + \beta_k(\omega^k - \omega^{k-1})\right)\right\}. \tag{9}$$

To simplify this procedure the coefficients α_k, β_k are chosen within $0 < \alpha \le 1$, $0 \le \beta < 1$. Then the conjugate gradient method (8) reduces to the heavy ball method [11].

The coefficients Δv, a' are calculated by using procedure (8). For the case shown in Fig. 1, the procedure (8) yields the synthetic antenna pattern shown in Fig. 4. It takes 36 iterations only at $\alpha = 0{,}9$, $\beta = 0{,}2$. The result is shown in Fig. 4.

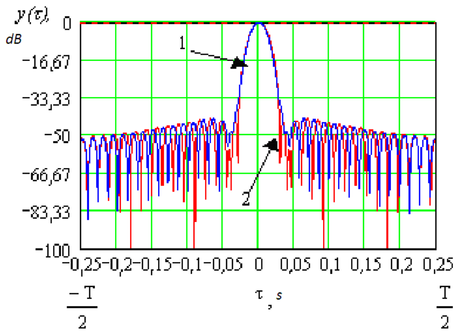

Fig. 4 The corrected synthetic antenna pattern (curve 1), ideal synthetic antenna pattern (curve 2)

As seen from Fig. 4, the main lobes of both corrected and ideal patterns are equal, but side lobes are not. One can find the residual approximation error at the level minus 50 dB. This error results from the calculation errors of correcting coefficients. This is quite sufficient for most practical applications.

IV. RESULTS

An effect of using the adaptive correction of an image acquired in synthesizing a hologram of the decimetric-band SAR ($\lambda = 0.23$ m) is visible when comparing the images shown in Figs. 5 and 6.

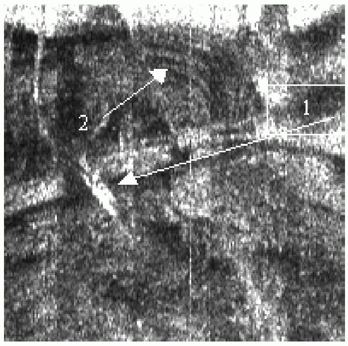

Fig. 5 The fragment of the uncorrected synthesized image during aircraft maneuvering

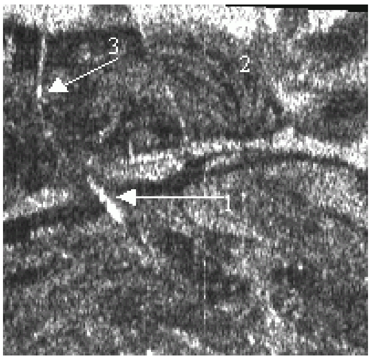

Fig. 6 The fragment of the corrected synthesized image during aircraft maneuvering

Specifically, as a result of adaptive correction of the supporting function in (1) the repeated object 1 in Fig. 5 has been removed (see Fig. 6). The periodical structure on both images (marked by digit 2 in Figs. 5 and 6) was unchanged. It is evident that this object is real. To calculate the correction coefficients we used the estimates of Doppler spectrum as shown in Fig. 3.

Figs. 7 and 8 show the results of signal processing by the proposed method for metric-band SAR ($\lambda = 1{,}8$ m). In Figs. 5-8 the azimuthal direction is shown from top to bottom, and the direction along the slant range – from left-hand to right-hand. The slant range resolution for the decimetric-band SAR is 22.5 m, and in the azimuthal direction – 10 m. The resolution sell for images was 15 x 37.5 m in Figs. 7 and 8.

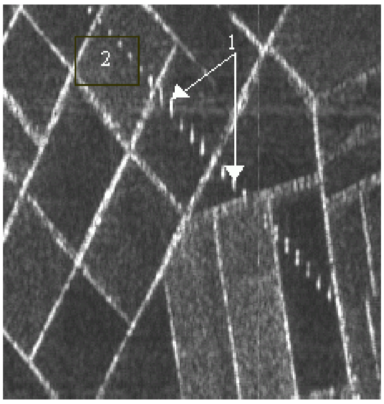

Fig. 7 The fragment of the uncorrected synthesized image during aircraft maneuvering

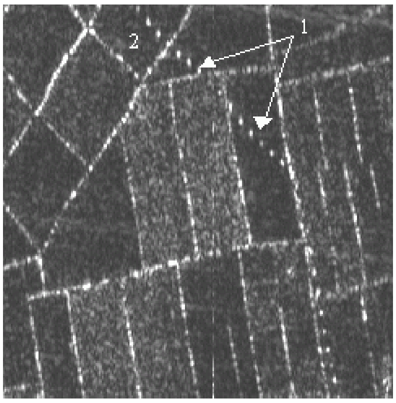

Fig. 8 The fragment of the corrected synthesized image during aircraft maneuvering

In Fig. 7 one can see the defocused-in-azimuth plane dots which are the columns (marked by digit 1) of electricity transmission lines. In Fig.8 shown after correcting the synthesized image the same strip has objects like normal targets (marked by digit 2). Besides, the bright solid lines that correspond to the forest belts are well-defined in Fig. 8 and appear to be more detailed as compared to Fig. 7.

Apart from the visual estimate of quality correction of the synthesized images the quantitative criteria can be used for image analysis. As a criterion, we suggested using the comparative analysis of radar's contrasts along the data row during the flight. For instance, Fig. 9 presents the results obtained from synthesizing one row of azimuth uncorrected data and in Fig. 10 the result of synthesis of the same data using the proposed correction algorithm.

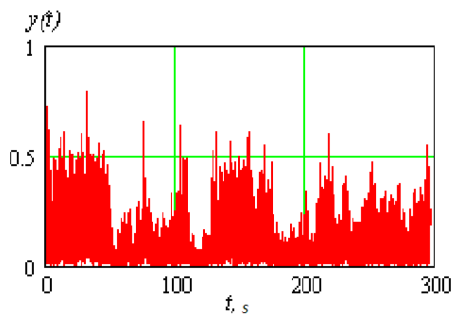

Fig. 9 The result from synthesizing one row of uncorrected azimuth data

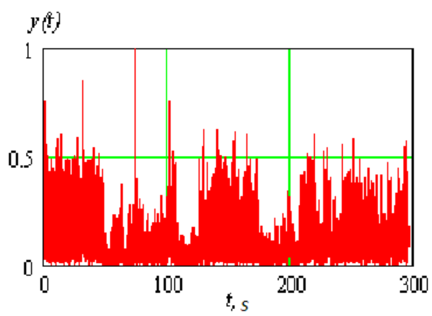

Fig. 10 The result from synthesizing one row of corrected azimuth data

For convenience of comparison, the scale of amplitudes of response from target along the ordinate axis in Figs. 9 and 10 is linear, whereas the amplitudes of responses are normalized to maximum in Fig. 10.

The total time of data recording was 300 seconds at flight velocity of 487 km/h. The slant range to a strobe was 13680 m, and the synthesizing interval was 1.8 seconds.

The adaptive correction algorithm was used during the whole flight and, as a result, one can see the growth of image contrasts, in the average, approximately at 10– 20 %, and for a separate target (for example, the target within an interval of 70 and 90 seconds, see Fig. 10) the response amplitude has increased by a factor of almost 1.5.

The generalized block diagram of the adaptive correction algorithm is shown in Fig. 11.

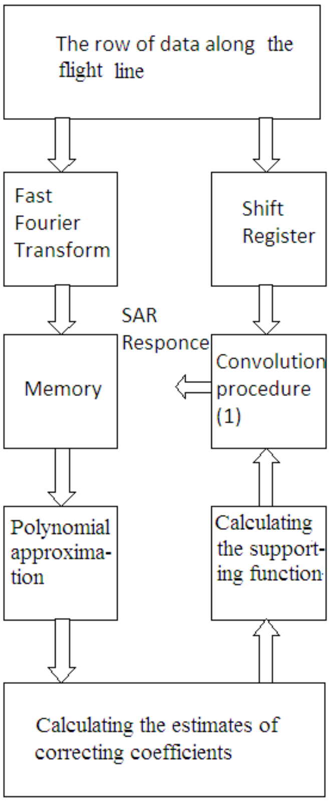

Fig. 11 The generalized block diagram of the adaptive correction algorithm

The procedure for processing the distorted parts of ground surface image is as follows: the initial coherent trajectory signal data is pre-processed by Fourier transform and the trajectory signal samples are concurrently stored on shift registers.

Averaging several adjacent slant range strobes is used to reduce the dispersion of spectrum samples. The spectral estimate thus obtained is polynomially approximated. The resulting polynom is investigated on an extremum by means of the recursive two-step procedure. This procedure has been chosen in an effort to find a compromise between the convergence rate and the computations per step of one iteration.

V. CONCLUSIONS

Thus, we have succeeded in building the adaptive correction algorithm for trajectory errors caused by maneuvering the SAR platform. As a consequence, we had to augment the computations (approximately by 30% per each synthesizing interval).

Theory and practice of using this adaptive algorithm has shown that azimuth resolution on separate areas of SAR images can be increased twice and the amplitudes of responses from some targets have grown by a factor of 1.5. The convergence rate of the recurrent procedure is proportional to geometric progression, and in each case it depends upon the initial shifts from an extremum and the value of fluctuation component Doppler spectrum dispersion. The algorithm allowed calculates the appropriate estimates of flight velocity errors and aircraft acceleration for 30 — 40 iterations for a real row of data presented in this paper. Accelerating the calculation rate is made possible by optimizing the parameters α_k, β_k in procedure (8).

REFERENCES

[1] Radars with Digital Synthesis of Antenna Aperture / Edit. V.Goryainov – Moscow, 1988, p. 304. (in Russian).

[2] K. Tomiyasu Tutorial Review of Synthetic Aperture Radar (SAR) with Applications to Image of Ocean Surface // *Proc. IEEE 66*, pp.

563-583 (1978).

[3] Ya. Itshoky, N. Sazonov, Ye. Tolstov Main Characteristics of SAR under Arbitrary Platform Motion // *Radiotehnika and Electronica*. - 1984., №11, pp. 2164-2172 (in Russian).

[4] Hounam D., Motion Errors and Compensation Possibilities // *AGARD Lecture Series 182. Fundamentals and Special Problems of Synthetic Aperture Radar (SAR)*.1992, pp. 31-42.

[5] Moreira J.A. A New Method of Aircraft Motion Error Extraction from Radar Raw Data for Real Time SAR Motion Compensation. // *Proc., IGARSS Symposium*, Vancover, Canada. 1999, pp. 1-7.

[6] O. Sytnik, The criteria of image quality of coherent radars // «*Kosmitchna nauka and Technology*». 2002. 8, №2/3, pp. 287-288. (in Russian).

[7] Cumming I., Wong F., Hawkins R., RADARSAT-1 Doppler Centroid Estimation Using Phase Based Estimators // *Proc., IGARSS Symposium*, 2002, pp. 1-3.

[8] Sharif A. H. A., Cumming I. Centroid Estimation for Azimuth-Offset SARs // *Proceedings of the IEEE National Aerospace and Electronics Conference, NAECON'95*, 1995, Dayton, Ohio, May 22-26, pp. 134-139.

[9] S. Lawrence Marple, JR., Digital Spectral Analysis with Applications // *Prentice-Hall, Englewood Cliffs, N. J.,* 1987, p. 492.

[10] Korn, G. A. and Korn, T. M., Mathematical Handbook for Scientists and Engineers, Second Edition, Dover, New York, 2000.

[11] B. Polyak, Introduction in Optimization Theory. – Moscow, 1983, p. 384. (in Russian).

Oleg Sytnik was born in Dneprodzerginsk, Ukraine, on May 17, 1958. He received an M.S. degree in radio engineering from the Kharkov University of Radio Electronics, Kharkov in 1980. He worked in the Design Bureau of Machine-Building Plant of Dnipropetrovsk (1980-1982), and then at the Radio Engineering Department of the Kharkov University of Radio Electronics (1982-1986). He received a Ph.D. degree in Radar and Navigation from the Kharkov University of Radio Electronics, Kharkov, in 1986. Since 1986 he has worked as a senior researcher at the A. Ya. Usikov Institute for Radio Physics and Electronics under the National Academy of Sciences of Ukraine in the Department of Radiophysical Introscopy and in the A.I. Kalmykov Center for Remote Sensing of the Earth under the Space Agency of Ukraine. During this time he received a Doctor of Sciences degree in Radio Physics and Mathematics as well as a Professorship (2005). He has published over 150 science papers on radar theory, digital signal processing and applications. His fields of research are radar, digital signal and image processing, pattern recognition and stochastic non-stationary processes.